**Adam MUC[1], Jan IWASZKIEWICZ[2]**

Uniwersytet Morski w Gdyni, Katedra Automatyki Okrętowej (1, 2)
ORCID: 1. 0000-0002-9495-087X; 2. 0000-0002-9827-715X

doi:10.15199/48.2023.09.42

# Scalar Voltage-Frequency Control of the OVT Inverter

***Abstract**. The paper presents the possibility of the scalar output voltage control of an OVT inverter. The OVT inverter is built of two component two-level three-phase inverters: the main inverter (MI) and the auxiliary one (AI). The idea of the OVT inverter control and construction is based on the orthogonal space vectors theory. The output voltage of the OVT inverter takes the shape of a stepped voltage analogous to the voltage generated by multilevel inverters. The paper demonstrates possible control methods of the output voltage frequency and amplitude. The results obtained during simulation studies prove that the output voltage essential parameters may be a function of the DC voltage and the control circuitry permits easy defining of selected voltage/frequency characteristics.*

***Streszczenie.** W artykule przedstawiono sposób sterowania skalarnego napięcia i częstotliwości falownika napięcia w oparciu o teorię przestrzennych wektorów ortogonalnych (OVT). Falownik OVT zbudowany jest z dwóch składowych dwupoziomowych falowników trójfazowych: falownika głównego (MI) i pomocniczego (AI). Napięcie wyjściowe falownika OVT ma postać napięcia schodkowego analogicznego do napięcia generowanego przez falowniki wielopoziomowe. W artykule przedstawiono możliwe metody sterowania częstotliwością i amplitudą napięcia wyjściowego. Uzyskane wyniki badań symulacyjnych dowodzą, że istotne parametry napięcia wyjściowego mogą być funkcją napięcia stałego zasilającego falowniki, a układ sterowania pozwala na łatwe definiowanie charakterystyk napięciowo-częstotliwościowych. **(Skalarne sterowanie napięciowo-częstotliwościowe falownika OVT**).*

**Keywords**: space vector; vector orthogonality; three-phase OVT inverter; fundamental harmonic.
**Słowa kluczowe**: wektor stanów, wektor ortogonalny, trójfazowy falownik OVT, harmoniczna podstawowa.

## Introduction

The conversion DC/AC direct into alternating current is one of the most essential targets of contemporary power electronics. Such a necessity is required in AC drives as well as in the area of renewable energy applications e.g. smart grids. In both domains, the critical parameters that should be regulated are voltage amplitude and frequency although the regulation range of these parameters is quite different. A typical control system applied in AC drives includes an inverter acting as a DC/AC converter. The most practical control method PWM (pulse-width modulation) causes the output voltage takes the form of rectangular pulses. Therefore, in order to receive a sine wave voltage, it is usually obligatory to use a low band filter which is capable to select a fundamental harmonic voltage component.

There are many thinkable sources of DC voltage. Three diversified examples of the DC/DC conversion in regard to their principle of operation have been presented in [1–3]. They are able to deliver a very high voltage gain; therefore, they are particularly suitable for use as an interface between photovoltaic sources and the grid. Additional applicable DC/DC converters designed to be used in fuel cell power systems are also greatly discussed [4–6]. They generate the DC voltage to supply inverters forming the DC/AC conversion.

The OVT subject inverter might be numbered to multilevel inverters because it generates a relatively reduced amount of output voltage harmonics [7], so the OVT inverter is very suitable to apply as an interface between DC sources and the smart grid. Multilevel inverters as well as multi-input converters are efficient devices for grid-connected hybrid PV or wind power systems [8].

If the OVT inverter works as an interfacing device standard control methods such as PWM or SVCM (space vector control method) are not particularly effective because the output voltage is formed as a sequence of rectangular and diversified in width steep pulses and comprises a great content of higher harmonics (high THDU). For this reason, an alternative based on the amplitude modulation method (AM) of the inverter output voltage has been carefully considered. As a consequence, there are proposals devoted to solutions based on the AM control method. They generally relate to multilevel inverters and many of them have been designed as grid-connected inverters acting also as the interface between photovoltaic systems and the grid network [9–12].

The simplest way to control the VSI is to switch every 60° appropriate transistor pairs of the two-level inverter. Then, the VSI generates a phase voltage that varies stepwise. This method of voltage generation has some advantages, including a simple control system and high efficiency of the inverter due to the negligible switching losses. What is more the ratio of the fundamental harmonic frequency to the switching frequency is equal to 6 and relatively high compared to other control methods. The modulation index expressing the relation UD/Uh1 is the highest in two-level inverters. The biggest disadvantage of such a control method is the considerable content of harmonics in the output stepwise voltage. For example, the total harmonic distortion factor ($THD_U$) in a single-phase inverter controlled in this way is approximately 31%. In addition, it is not easy to regulate the fundamental harmonic value of the output voltage. In this case, it is necessary to adjust the UD voltage supplying the inverter or to use other methods. Therefore, this control method is rarely used in practice, although its weaknesses are diminished in multiphase inverters.

However, there are some stimulating possibilities concerning DC/AC converters constructed of two two-level inverters, which are considered, for the purposes of this paper, as orthogonal-vectors-controlled inverters (OVTs). The main advantages and disadvantages of the control concept based on orthogonal vectors have been presented and discussed in [13, 14, 15, 16]. The original control method of the auxiliary inverter didn't remain very efficient. The use of a transformer transferring relatively long pulses was the main disadvantage of the presented solution. A novel idea of the auxiliary inverter control method has been developed and described in [17]. This paper presents a novel, modified proposal regarding the OVT inverter control method. The recommended control method brought a significant reduction in the transformer size used as a summing node of the OVT inverter.

## The OVT inverter idea

The basic block diagram of the OVT inverter is shown in Figure 1. The idea and performance of the inverter have been developed and presented in the aforementioned publications [13, 14, 15, 16] as well as the modified proposal [17]. Built from two standard two-level inverters: a main inverter (MI) and an auxiliary one (AI) the OVT inverter generates 18 similar in-length space voltage vectors. The component inverters are specifically connected and supplied from one DC voltage source. The block diagram is presented in Figure 1. Next figure 2 determines the rule of vector creation. The vectors are denoted as:

- $V_{MIk}$ — the main inverter voltage vector k;
- $V_{AIk}$ —the auxiliary inverter voltage vector k;
- $V_{OVTk}$ — the OVT inverter voltage vector k

and k = 1, 2, 3, 4, 5, 6.

The vectors $V_{MIk}$ and $V_{AIk}$ are mutually orthogonal and presented in Figure 3.

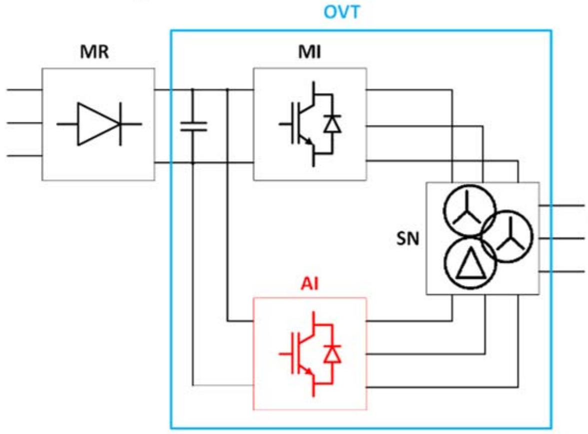


Fig.1. Scheme the OVT inverter, where: MI – main inverter, AI – auxiliary inverter, OVT – orthogonal vector cotntrol inverter, SN – sum node, MR - main rectifier

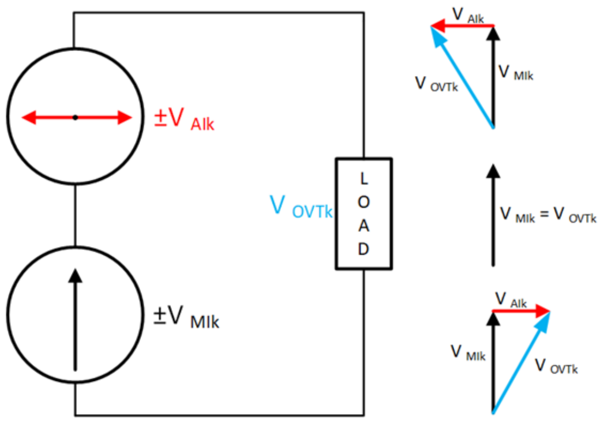


Fig.2. The formation concept of vectors $V_{OVTk}$

In every of six k-sectors of the stationary coordinate system plane (α, β) the OVT inverter generates a sequence of three voltage vectors: V_(OVT-), V_OVT, V_(OVT+), assigned to the k-th sector of the plane (α, β). The order of generation is described in equation (1):

$$
(1)\qquad
\begin{aligned}
\vec{\boldsymbol{V}}_{Ok-} &= \vec{\boldsymbol{V}}_{Ak\oplus 3} + \vec{\boldsymbol{V}}_{Mk} \\
\vec{\boldsymbol{V}}_{Ok} &= \vec{\boldsymbol{V}}_{Mk} \\
\vec{\boldsymbol{V}}_{Ok+} &= \vec{\boldsymbol{V}}_{Ak} + \vec{\boldsymbol{V}}_{Mk}
\end{aligned}
$$

The symbol k⊕3 denotes the modulo 6 sum of the index k and the number 3. Expression (1) illustrates a control method based on the principle of orthogonal vector summation. In the stationary coordinate system (α, β) the active vectors of the component inverters are described by expressions (2).

$$
(2)\qquad
\begin{cases}
\vec{\boldsymbol{V}}_{Mk} = \left|\vec{\boldsymbol{V}}_{Mk}\right| e^{j\left[(k-1)\frac{\pi}{3} \pm 2\pi n\right]} \\
\vec{\boldsymbol{V}}_{Ak} = \pm jm\,\vec{\boldsymbol{V}}_{Mk} = \pm m\,\vec{\boldsymbol{V}}_{Mk}\, e^{j\frac{\pi}{2}}
\end{cases}
$$

where: k = 1, 2, 3, 4, 5, 6 ; n = 1, 2, 3, ... .

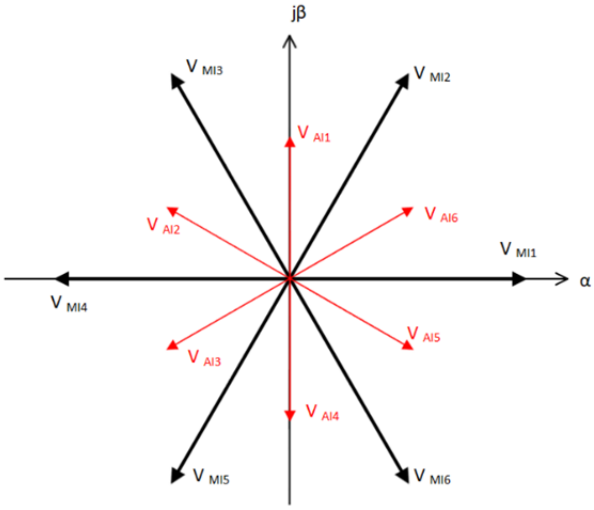


Fig.3. The active vectors of the main and auxiliary inverters

The factor m is the ratio of the moduli (lengths) of the vectors (3).

$$
(3)\qquad \boldsymbol{m} = \frac{\left|\vec{\boldsymbol{V}}_{Ak}\right|}{\left|\vec{\boldsymbol{V}}_{Mk}\right|}
$$

According to equations (1, 2), the output space vectors of the OVT orthogonal converter are given by relations (4).

$$
(4)\qquad
\begin{cases}
\vec{\boldsymbol{V}}_{Ok-} = (1 - jm)\,\vec{\boldsymbol{V}}_{Mk} = \sqrt{1+m^2}\,\vec{\boldsymbol{V}}_{Mk}\, e^{-j\cdot \arctan m} \\
\vec{\boldsymbol{V}}_{Ok} = \vec{\boldsymbol{V}}_{Mk} = \left|\vec{V}_{Mk}\right| e^{j\left[(k-1)\frac{\pi}{3} \pm 2k\,\pi\right]} \\
\vec{\boldsymbol{V}}_{Ok+} = (1 + jm)\,\vec{\boldsymbol{V}}_{Mk} = \sqrt{1+m^2}\,\vec{\boldsymbol{V}}_{Mk}\, e^{\,j\cdot \arctan m}
\end{cases}
$$

If it is assumed that the output vectors are switched on at equal time intervals, the ratio of the lengths of the vectors is equal to (5).

$$
(5)\qquad m = \frac{\left|\vec{\boldsymbol{V}}_{Ak}\right|}{\left|\vec{\boldsymbol{V}}_{Mk}\right|} = tg\left(\frac{\pi}{9}\right) = 0.364
$$

Figure 4 shows a summary of the control vectors for the main and auxiliary inverters. Along with the vectors, the theoretical waveforms of the phase-to-phase voltages for each inverter are shown. In the basic configuration, the main inverter is connected to the load in a star configuration, while the auxiliary inverter is connected by use of a transformer working in delta-star configuration. Figure 4 shows that the vectors of the auxiliary inverter are generated three times frequently in one sector of the (α, β) plan, so the vector frequency of the AI is three times higher in relation to the vector frequency of the MI.

a)

| | 1 | 2 | 3 | 4 | 5 | 6 | 7 | 8 | 9 | 10 | 11 | 12 | 13 | 14 | 15 | 16 | 17 | 18 |
|---|---|---|---|---|---|---|---|---|---|---|---|---|---|---|---|---|---|---|
| vectors / phases | v5 | v5 | v5 | v4 | v4 | v4 | v6 | v6 | v6 | v2 | v2 | v2 | v3 | v3 | v3 | v1 | v1 | v1 |
| a | 1 | 1 | 1 | 1 | 1 | 1 | 1 | 1 | 1 | 0 | 0 | 0 | 0 | 0 | 0 | 0 | 0 | 0 |
| b | 0 | 0 | 0 | 0 | 0 | 0 | 1 | 1 | 1 | 1 | 1 | 1 | 1 | 1 | 1 | 0 | 0 | 0 |
| c | 1 | 1 | 1 | 0 | 0 | 0 | 0 | 0 | 0 | 0 | 0 | 0 | 1 | 1 | 1 | 1 | 1 | 1 |

b)

| | 1 | 2 | 3 | 4 | 5 | 6 | 7 | 8 | 9 | 10 | 11 | 12 | 13 | 14 | 15 | 16 | 17 | 18 |
|---|---|---|---|---|---|---|---|---|---|---|---|---|---|---|---|---|---|---|
| vectors / phases | v3 | v7 | v4 | v1 | v0 | v6 | v5 | v7 | v2 | v4 | v0 | v3 | v6 | v0 | v1 | v2 | v0 | v5 |
| a | 0 | 1 | 1 | 0 | 0 | 1 | 1 | 1 | 0 | 1 | 0 | 0 | 1 | 1 | 0 | 0 | 0 | 1 |
| b | 1 | 1 | 0 | 0 | 0 | 1 | 0 | 1 | 1 | 0 | 0 | 1 | 1 | 1 | 0 | 1 | 0 | 0 |
| c | 1 | 1 | 0 | 1 | 0 | 0 | 1 | 1 | 0 | 0 | 0 | 1 | 0 | 1 | 1 | 0 | 0 | 1 |

Fig.4. The theoretical waveforms (in black) of the phase-to-phase voltages corresponding to the control vectors for the main (a) and auxiliary inverters (b).

## Simulation model and operation principle

Scalar control algorithm u/f = constant applied to the OVT inverter needs an additional converter who works as a rectifier providing the DC voltage to supply the OVT. The PWM control method is not used in OVT inverters because the idea of their operation is based on the assumption that the MI is switched possibly infrequently. The whole strategy of control is created on cyclical switching of defined vector sequences according to the rule presented in Figure 4. The auxiliary inverter AI is controlled synchronously to the MI and it acts as an active filter of the MI output voltage. Both inverters are DC voltage supplied, so it is easy to control the output voltage frequency and it's impossible to adjust the output voltage level. In order to achieve this property a thyristor-controlled rectifier has been used. Therefore the output average voltage of the rectifier depends on the control angle. An additional gamma filter, built from LD and CD elements, is connected to the rectifier output. The complete converter diagram is presented in Figure 5.

Realization of the u/f characteristic has the need for a specialized control system. Its goal is to synchronize both MI and AI inverters according to the set output voltage frequency. At the same time, it has to synchronize the thyristor rectifier's operation. The block denoted as 6-pulse generator obtains mains synchronous signals to the input phi from the PLL (phase locked loop) block. The alpha input of the block acquires calculated thyristor phase angles according to the function set into the block Fcn.

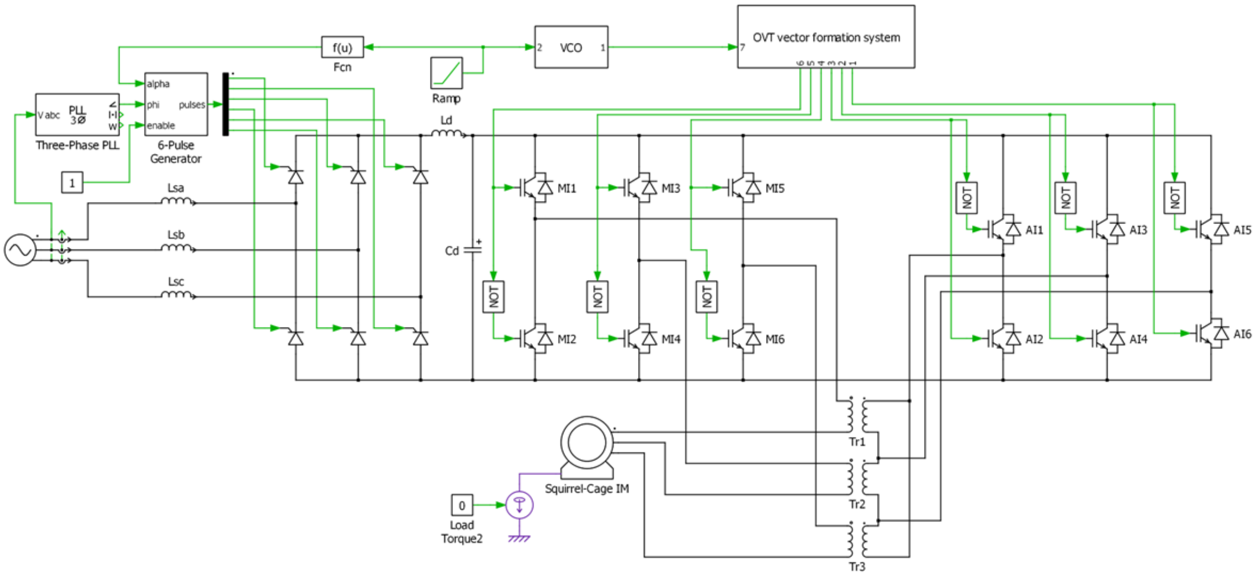


Fig.5. The complete converter diagram under simulation tests

## Results of simulation tests

Simulation tests were performed in the PLECS program and the RT Box device. The PLECS program is a dedicated program for modeling power electronic converters, while the RT Box is a device that allows conducting simulation tests in the hardware loop (HIL).

Simulation tests were performed in a wide range of frequencies and speeds for the induction motor. The adopted motor model corresponds to the power of 4 kW, and its detailed parameters are presented in table 1.

Tabela 1. Induction motor parameters

| Parameters | | Value |
|---|---|---|
| Pn | [VA] | 4000 |
| Vn | [Vrms] | 400 |
| fn | [Hz] | 50 |
| Rs | [ohm] | 1.405 |
| Lls | [H] | 0.005839 |
| Rr' | [ohm] | 1.395 |
| Llr' | [H] | 0.005839 |
| Lm | [H] | 0.1722 |
| J | [kg m^2] | 0.0131 |
| F | [N.m.s] | 0.002985 |
| p | - | 2 |

Figure 6 shows the waveforms of voltages, currents and changes in the motor rotation speed for the frequencies of 20 Hz and 50 Hz. For the assumed frequencies, the engine revolutions varied from 8000 rpm to 1400 rpm.

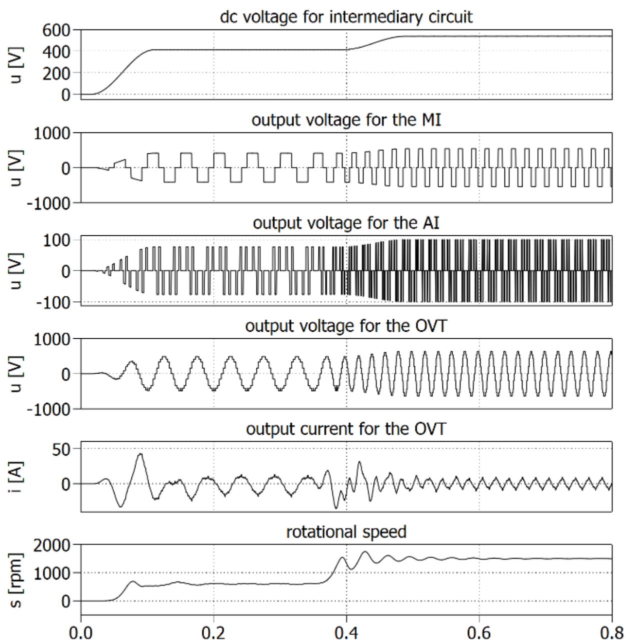


Fig.6. Voltage, current and speed waveforms for an orthogonal inverter feeding a 4 kW induction motor

The figures 7 and 8 shows the spectra for the tested operating frequencies of the converter.

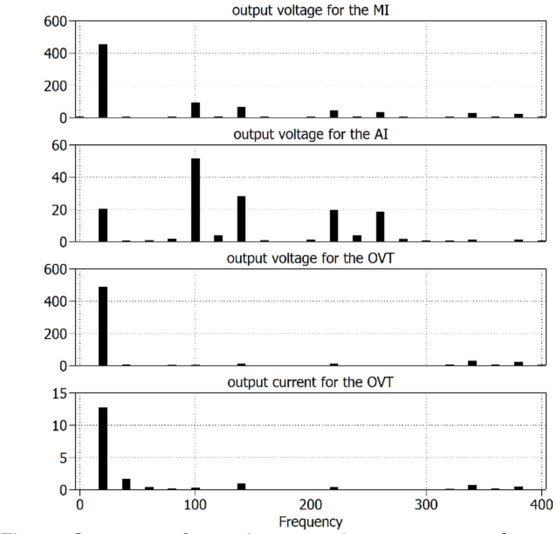


Fig.7. Spectrum for voltage and current waveforms with a frequency of 20 Hz

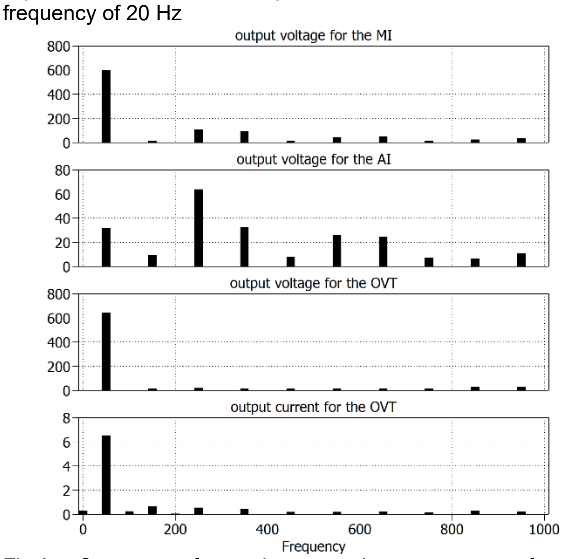


Fig.8. Spectrum for voltage and current waveforms with a frequency of 50 Hz

The spectra presented in Figures 7 and 8, especially concerning the output voltage and current waveforms, are characterized by the presence of only the fundamental harmonic. This effect was achieved without the use of PWM modulation.

**Conclusions**

The presented OVT inverter is designed to support an efficient DC/AC conversion process. The total power of the OVT inverter can be very high, as can the MI power, but the power of the AI inverter remains relatively low. As a result, the power losses of the entire OVT inverter, as well as the MI and AI component inverters, are very low. The MI main inverter is switched only six times per period of harmonic voltage and AI power losses correspond to approximately only 5% ÷ 7% of the MI losses. This allows the control circuit of the complete OVT inverter to operate in the simplest way. Simulation results demonstrate that the OVT inverter is capable to control the frequency and amplitude of the output voltage simultaneously, but requires a controlled DC voltage source. The relevant parameters of the OVT output voltage can be a function of the DC voltage level, and the control circuit allows the selection of voltage/frequency characteristics to be easily defined. The THD coefficients of voltage and current meet the limits of EN: 50160.

*Funding: This project is financially supported under the framework of a program of the Ministry of Science and Higher Education (Poland) as “Regional Excellence Initiative” in the years 2019–2022, project number 006/RID/2018/19, amount of funding 11 870 000 PLN.*

***Authors**: dr hab. inż. Jan Iwaszkiewicz, E-mail: j.iwaszkiewicz@we.umg.edu.pl; dr inż. Adam Muc, E-mail: a.muc@we.umg.edu.pl; Uniwersytet Morski w Gdyni, Katedra Automatyki Okrętowej, Wydział Elektryczny, ul. Morska 81-87, 81-225 Gdynia.*

REFERENCES

[1] H.L. Do, A Soft-Switching DC/DC Converter with High Voltage Gain. IEEE Trans. Power Electron. 2010, 25, pp.1193–1200, https://doi.org/10.1109/TPEL.2009.2039879
[2] R. Wai, S. Member, C. Lin, R. Duan, Y. Chang, High-Efficiency DC-DC Converter With High Voltage Gain 437 and Reduced Switch Stress. IEEE Trans. Ind. Electron. 2007, 54, pp. 354–364
[3] X. Hu, J. Wang, L. Li, Y. Li, A Three-Winding Coupled-Inductor DC–DC Converter Topology With High Voltage Gain and Reduced Switch Stress. IEEE Trans. Power Electron. 2018, 33, 1453–1462 https://doi.org/10.1109/TPEL.2017.2689806.
[4] K. Jin, X Ruan, Hybrid Full-Bridge Three-Level LLC Resonant Converter—A Novel DC–DC Converter Suitable for Fuel-Cell Power System. In Proceedings of the 2005 IEEE 36th Power Electronics Specialists Conference, Dresden, Germany, 16 June 2005; Volume 53, pp. 1492–1503
[5] H. Ramirez, C. Restrepo, T. Konjedic, J. Calvente, A. Romero, C. Baier, R. Giral, Efficiency Comparison of Fuel-Cell Hybrid Systems Based on the Noninverting Buck-Boost Converter. IEEE Trans. Power Electron. 2017, 33, pp. 1237–1246
[6] M.D. Siddique, Low Switching Frequency Based on Asymmetrical Multilevel Inverter Topology With Reduced Switch Count. IEEE Access 2019, 7, pp. 86374–86383.
[7] J. Iwaszkiewicz, J. Perz, Multilevel Convertors for istributed Power Generation Systems with DC Voltage Sources; ICREPQ: Saragossa, Spain, 2005
[8] Y.M. Chen, Y.C. Liu, S.C. Hung, C.S. Cheng, Multi-input inverter for grid-connected hybrid PV/wind power system. IEEE Trans. Power Electron. 2007, 22, pp. 1070–1077
[9] N.A. Rahim, K. Chaniago, J. Selvaraj, Single-Phase Seven-Level Grid Connected Inverter for Photovoltaic System. IEEE Trans. Ind. Electron. 2011, 58, 2435–2443
[10] J. Liu, X. Zhu, J. Zeng, A Seven-level Inverter with Self-balancing and Low Voltage Stress. IEEE J. Emerg. Sel.Top. Power Electron. 2018, 8, 685–696
[11] P. Roshankumar, R.S. Kaarthik, K. Gopakumar, J.I. Leon, A Seventeen-Level Inverter formed by Cascading Flying Capacitor and Floating Capacitor H-bridges. IEEE Trans. Power Electron. 2014, 30, 3471–3478
[12] E. Drives, A. Maather, P. Electronics, N. Ouest, A Novel 31-Level Packed U Cells Converter. In Proceedings of the 2011 International Conference on Power Engineering, Energy and Electrical Drives, Malaga, Spain, 11–13 May 2011
[13] M. Hartman, M. Hashad, J. Iwaszkiewicz, Developing Inverter Output Voltage Waveforms with the Help of Orthogonal Space Vectors, IEE Conference Power Electronics and Variable Speed Drives PEVD’2000, London, United Kingdom, 18–19 IX 2000
[14] M. Hashad, J. Iwaszkiewicz, A Novel Orthogonal-Vectors-Based Topology of Multilevel Inverters. IEEE Trans. Ind. Electron. 2002, 49, pp. 868–874
[15] J. Iwaszkiewicz, A Novel Recurrent Approach to the Output Voltage Filtering of the Inverter. Electr. Power Qual. Util. Pol. Acad. Sci. 2003, 9, pp. 59–65
[16] J. Iwaszkiewicz, A. Muc, The active filtering of the inverter output voltage by use of orthogonal vectors’ control strategy, Renewable Energy and Power Quality Journal, 2022, No. 20, pp. 817-821, https://doi.org/10.24084/repqj20.446
[17] A. Muc, J. Iwaszkiewicz, Active Filtering of Inverter Output Waveforms Based on Orthogonal Space Vector Theory, Energies 2022, 15(21), 7861, https://doi.org/10.3390/en15217861